

Brief Communication

Vascular endothelial growth factor C therapy for polycystic kidney diseases

Jennifer L Huang¹, Adrian S Woolf², Maria Kolatsi-Joannou¹, Peter Baluk³, Richard N Sandford⁴, Dorien JM Peters⁵, Donald M McDonald³, Karen L Price¹, Paul JD Winyard¹, David A Long¹

¹Developmental Biology and Cancer Programme, UCL Institute of Child Health, London, WC1N 1EH, UK.

²Institute of Human Development, Faculty of Medical and Human Sciences, University of Manchester, M13 9PT, UK.

³Cardiovascular Research Institute, Comprehensive Cancer Centre, and Department of Anatomy, University of California, San Francisco, California, USA.

⁴Academic Department of Medical Genetics, University of Cambridge School of Clinical Medicine, Cambridge, CB2 0SP, UK.

⁵Department of Human Genetics, Leiden University Medical Centre, Leiden, The Netherlands.

Corresponding Author

David A Long PhD, Developmental Biology and Cancer Programme,
UCL Institute of Child Health, 30 Guilford Street, London, WC1N 1EH, UK.

Tel: +44 (0)207 905 2615;

Fax: +44 (0)207 905 2133;

E-mail: d.long@ucl.ac.uk

Running Title: VEGFC therapy for PKD

Word Count: Abstract: 238 Text: 1936 (excluding methods, references and legends)

Abstract

Polycystic kidney diseases (PKD) are genetic disorders characterised by progressive epithelial cyst growth leading to destruction of normal functioning renal tissue. Current therapies have focussed on the cyst epithelium and little is known about how the blood and lymphatic microvasculature may modulate cystogenesis. In hypomorphic *Pkd1^{nl/nl}* mice cystogenesis was associated with a disorganised pericyclic network of vessels expressing platelet/endothelial cell adhesion molecule 1 and vascular endothelial growth factor (VEGF) receptor 3. The major ligand for VEGFR3 is VEGFC and we found reduced production of *Vegfc* mRNA within the kidneys during the early stages of cystogenesis in seven day old postnatal *Pkd1^{nl/nl}* kidneys. We therefore treated the mice with exogenous VEGFC on the premise that this would remodel both the VEGFR3⁺ pericyclic vascular network and larger renal lymphatics which may also impact on the severity of PKD. VEGFC enhanced VEGFR3 phosphorylation in the kidney, normalised the pattern of the pericyclic network of vessels, widened the large lymphatics and this was associated with a significant reduction in cystic disease, blood urea nitrogen and serum creatinine. Furthermore, VEGFC reduced M2 macrophage pericyclic infiltrate which has been implicated in the progression of PKD. VEGFC administration also improved cystic disease in *Cys1^{cpk/cpk}* mice, a model of autosomal recessive PKD, leading to a modest but significant increase in lifespan. Overall, this study highlights VEGFC as a potential new treatment for some aspects of PKD, with the potential for synergy with current epithelial-targeted approaches.

Polycystic kidney diseases (PKDs) are genetic disorders, usually caused by mutations affecting proteins located in primary cilia and other regions within epithelial cells.¹ Epithelial turnover, adhesion, secretion, polarity and ciliary functions are altered in PKDs and therapies have predominantly targeted these processes.¹ Much less is known about how the blood and lymphatic microvasculature surrounding kidney tubules might modulate cystogenesis. Prior studies using corrosion casting and angiography showed that the vessels surrounding cysts in patients with autosomal dominant (AD)PKD are tortuous, abnormally patterned and dilated.^{2,3} Two further studies have blocked vascular endothelial growth factor A (VEGFA) signalling, a potent pro-angiogenic factor, in a non-orthologous rat PKD model but gave contradictory results and did not examine the effect of this intervention on the microvasculature.^{4,5}

We examined the blood and lymphatic microvasculature in *Pkd1^{nl/nl}* mice, which carry two hypomorphic alleles of *Pkd1*⁶ the mouse homologue of the gene most commonly mutated in human ADPKD. Small cysts were found in one day old *Pkd1^{nl/nl}* kidneys which become more prominent one week postnatally; larger cysts were observed at three weeks which reach a maximum at five weeks of age (**Figure 1A-E**). In wild-type mice, there was a fine reticular network of vessels around kidney tubules as identified by immunohistochemistry for a pan-endothelial marker, platelet/endothelial cell adhesion molecule 1 (CD31) (**Figure 1F,J**). In one day old littermate *Pkd1^{nl/nl}* mice there was an increase in the CD31⁺ area of non-cystic renal tissue (25.7%±4.9 and 38.9±0.7 in *Pkd1^{wt/wt}* and *Pkd1^{nl/nl}*, p<0.05, n=4/group) but no changes in the pattern of these vessels compared with *Pkd1^{wt/wt}* mice (**Figure 1G**). At three weeks of age, the pattern of CD31⁺ vessels was disrupted in *Pkd1^{nl/nl}* mice, with clusters of tortuous vessels around cysts (**Figure 1K**) and an increased percentage area compared with *Pkd1^{wt/wt}* animals (**Table S1**). Despite the increased relative area occupied by the vessels, proliferating (CD31⁺/Ki67⁺) endothelial cells per unit area were significantly reduced in PKD kidneys (**Table S1**).

Lymphatics were identified using a panel of markers including VEGF receptor 3 (VEGFR3), podoplanin (PDPN), lymphatic vessel endothelial hyaluronan receptor 1 (LYVE1) and prospero homeobox 1 (PROX1). All 4 proteins co-localised in large intrarenal periarterial lymphatics in both wild-type and *Pkd1^{nl/nl}* three week old kidneys and there was no change in transverse areas with PKD (**Figure S1, Table S1**). Intriguingly, we noted a second population of VEGFR3⁺ vessels that were negative for LYVE1, PDPN and PROX1. These were widely distributed in peritubular areas in wild-type mice (**Figure 1H,L**). In one day postnatal *Pkd1^{nl/nl}* kidneys, the VEGFR3⁺ area of non-cystic renal tissue was increased (18.7%±1.9 and 27.4±3.7 in *Pkd1^{wt/wt}* and *Pkd1^{nl/nl}*, p<0.05, n=4/group) but with no apparent changes in the pattern of the vessels compared with *Pkd1^{wt/wt}* mice (**Figure 1I**). At three weeks of age, the pattern of the peritubular VEGFR3⁺ vessels in *Pkd1^{nl/nl}* was disorganised (**Figure 1M**) with increased percentage area (**Table S1**). The VEGFR3⁺ patterns mimicked the CD31⁺ distribution pattern and using double labelling we demonstrated co-localisation of CD31 and VEGFR3 in the same vessels in three week old wild-type and cystic mice (**Figure 1N-U**). We postulate that these CD31⁺/VEGFR3⁺ vessels may be a kidney-equivalent to specialised capillaries seen in endocrine glands,^{7,8} with molecular features shared with lymphatic endothelia and high permeability facilitating the reabsorption of glomerular filtrate into the circulation in healthy kidneys.⁹

Subsequently, we hypothesised that targeting the microvasculature may alter PKD. We decide to focus on VEGFC, which enhances growth, survival and migration of adult lymphatic endothelia through actions on VEGFR3 with lesser effects on blood vessels via VEGFR2.¹⁰⁻¹² VEGFC would not only target the disorganised VEGFR3⁺ pericycystic vessels but also the larger VEGFR3⁺ lymphatics allowing us to modulate both of these vessel types. Firstly, we examined endogenous *Vegfc* in *Pkd1^{nl/nl}* kidneys and found a significant decrease in *Vegfc* mRNA levels at day 7 (p<0.01) but no difference at day 14 or 21 compared with *Pkd1^{wt/wt}* mice (**Figure 2A**). We then provided exogenous VEGFC to seven day old *Pkd1^{wt/wt}* mice by administering 100 ng/g body weight of recombinant VEGFC or vehicle

intraperitoneally every day for two weeks (**Figure 2B**), a period where there is rapid growth in the size of *Pkd1^{nl/nl}* kidneys. (**Figure S2**). This dose has been used for VEGFA to promote renal angiogenesis¹³ and a higher dose (200 ng/g body weight) of VEGFC enhances VEGFR3 phosphorylation *in-vivo*.¹⁴ We found that VEGFC administration enhanced tyrosine phosphorylation of VEGFR3 in *Pkd1^{nl/nl}* kidneys versus those administered PBS (**Figure 2C**). VEGFC treated *Pkd1^{nl/nl}* mice had reduced severity of PKD as assessed by the external appearance of kidneys at autopsy (**Figure 2D**) and a significant approximate halving in kidney/body weight ratio (**Figure 2E**). *Pkd1^{nl/nl}* mice receiving VEGFC had similar body weights to those administered vehicle but their absolute kidney weights were about half that of the untreated PKD littermates (1.2g±0.3 and 0.6±0.2 in *Pkd1^{nl/nl}* administered PBS and VEGFC, p<0.05). Kidneys of VEGFC treated animals contained less prominent cysts by histology (**Figure 2F-I**) with significantly smaller average cyst size (**Figure 2J**). VEGFC did not alter blood urea nitrogen (BUN) and creatinine (**Figure 2K-L**) concentrations in *Pkd1^{wt/wt}* animals; both of these parameters were strikingly increased in *Pkd1^{nl/nl}* administered PBS which was attenuated by VEGFC treatment. As a potential confounder, BUN can be lowered if there is liver damage but VEGFC did not affect plasma alanine aminotransferase levels (**Figure 2M**). In addition, VEGFC administration did not alter the histology of the heart, lung, liver and spleen (**Figure 2N-U**).

VEGFC therapy had two effects on the vasculature in *Pkd1^{nl/nl}* mice. Firstly, it increased the numbers of VEGFR3⁺/Ki67⁺ and CD31⁺/Ki67⁺ proliferating endothelial cells per unit area (**Table S1**). The pattern (**Figure 3A-F**) and percentage area (**Table S1**) of the CD31⁺ and VEGFR3⁺ vessels in *Pkd1^{nl/nl}* treated with VEGFC was more like that observed in normal kidneys. Secondly, VEGFC significantly increased the transverse area of the larger LYVE1⁺/Prox1⁺ lymphatics in the kidney (**Table 1**). However, VEGFC treatment did not significantly alter endogenous kidney mRNA levels of *Vegfa*, *Vegfc*, *Vegfr2* or *Vegfr3* or protein levels of VEGFC (**Figure S3**).

Next, we examined if these changes in the blood and lymphatic microvasculature might correlate with the inflammatory milieu in PKD by examining CD206/Mrc1⁺ alternatively activated macrophages (M2) which have been functionally implicated in PKD cyst growth^{15,16}. VEGFC significantly reduced these cells in *Pkd1^{nl/nl}* mice (**Figure 3G-J**). Treatment also led to significantly lower renal *Mrc1* levels in *Pkd1^{nl/nl}* mice (**Figure 3K**) although the reduction of another M2 marker, arginase 1 (*Arg1*), did not reach significance (**Figure 3L**). In contrast, none of the M1 macrophage markers tested were affected by VEGFC administration (**Figure 3M,N**). Similarly, the extent of fibrosis was unaffected, as assessed by mRNA for collagen type III, alpha 1 (*Col3a1*) (**Figure 3O**).

The normalisation of the pericyclic network of vessels alongside reduced inflammatory macrophages suggest the microvasculature is the prime target of VEGFC therapy, but the same results might be generated as secondary effects if the growth factor acted directly on cystic epithelia. However, VEGFC did not alter proliferation in small cysts (< 0.01 mm²; 29 ± 6 versus 33 ± 3 proliferating nuclei/500 cells in *Pkd1^{nl/nl}* administered PBS and VEGFC) with few Ki67⁺ cells detected in cysts larger than this in all experimental groups. In contrast to previous reports,^{3,4,17} we could not detect the VEGFC receptors, VEGFR2 or VEGFR3, on the cyst epithelia by immunohistochemistry in multiple animals; contrasting markedly with clear expression in vessels on the same section (**Figure 3P,Q**). Hence, we conclude that the prime effects of VEGFC are likely to be vascular-targeted, although we cannot fully rule epithelial effects which could be evaluated using isolated cyst models. It will be worth re-examining the VEGFA pathway in future experiments too. Previous studies were done in Han:SPRD rats, a model which does not harbour a human PKD-relevant mutation,¹⁸ with anti-VEGFA antibody causing worse renal function and enhanced kidney injury in one laboratory⁵ whereas ribozymes to block VEGFR1 and VEGFR2 reducing cyst volume density and improved renal function in another.⁴ An explanation for these findings is that simply blocking VEGFA is known to cause profound glomerular changes¹⁹ and the effects on cystic tubules could be secondary to these. The blockade of VEGFR2 by ribozymes may

favour endogenous VEGFC binding to VEGFR3⁺ vessels which our study has shown to be beneficial.

We questioned whether the positive effects of VEGFC are specific for *Pkd1* mutants or have more widespread effects on cystogenesis by using congenital polycystic kidney (*Cys1^{cpk/cpk}*) mice. This model is non-orthologous, but provides a rapid phenocopy of the pathology of human autosomal recessive (AR)PKD with massive collecting duct cystogenesis leading to uremic death by 3 weeks of age.²⁰ Firstly, we examined 2 week old *Cys1^{cpk/cpk}* mice and found that the CD31⁺ and VEGFR3⁺ pericyclic network of vessels were also disorganised compared with *Cys1^{+/+}* mice and that both markers co-localised (**Figure S4**). The relative area occupied by the VEGFR3⁺ vessels was significantly increased in *Cys1^{cpk/cpk}* mice compared with wild-type littermates with a tendency for this to be the case for CD31⁺ vessels (**Table S2**). VEGFC was again provided daily from postnatal day seven to fourteen (**Figure 4A**); a phase where there is rapid growth in the size of *Cys1^{cpk/cpk}* kidneys (**Figure S3**). VEGFC administration to *Cys1^{cpk/cpk}* mice led to an improvement in gross morphology (**Figure 4B**) and a significant reduction in kidney/body weight ratio compared with those administered PBS (**Figure 4C**). *Cys1^{cpk/cpk}* receiving VEGFC had similar body weights to those administered PBS but had a significantly lower kidney weight (0.6g±0.1 and 0.5±0.1 in *Cys1^{cpk/cpk}* administered PBS and VEGFC, p<0.05). VEGFC treatment, did not, however, affect blood urea nitrogen concentration (**Figure 4D**). Kidneys of VEGFC treated *Cys1^{cpk/cpk}* mice had less prominent cysts (**Figure 4E-H**) with a significantly smaller average cyst size (**Figure 4I**). VEGFC increased the number of proliferating CD31⁺ and VEGFR3⁺ vessels in *Cys1^{cpk/cpk}* mice (**Table S2**) which was associated with a reduction in the VEGFR3⁺ percentage area (**Table S2**). VEGFC administration did not alter the average cross-sectional area of the larger LYVE1⁺/Prox1⁺ lymphatics in *Cys1^{cpk/cpk}* mice. Finally, VEGFC treatment led to a modest but significantly extended survival of one week in *Cys1^{cpk/cpk}* mice (**Figure 4J**).

In conclusion, this study shows that an abnormal pericyclic network of vessels is present from the early stages of PKD and becomes more disorganised as cystogenesis progresses. We have shown that intervening with VEGFC enhances the phosphorylation of VEGFR3 which has been shown to lead to the proliferation, migration and rearrangement of vessels.²¹ VEGFC treatment also reduces the severity of PKD which is associated with improving the pattern of the pericyclic vascular network, widening the large lymphatics and clearing inflammatory cells. The combination of these effects may have the potential to reduce edema which is a regular feature of PKD.²² We do not yet understand why the kidney microvasculature is abnormal in PKD. One reason is that the vessels are simply distorted as cysts grow. Alternatively, there may be intrinsic defects in the vasculature, as has been reported in the skin lymphatics in *Pkd1*- and *Pkd2*-null mice²² which may explain why the effects of VEGFC are more prominent in *Pkd1*^{nl/nl} mice than *Cys1*^{cpk/cpk}. Other studies have also demonstrated a role for *Pkd1* in zebrafish lymphatic vessel morphogenesis²³

Future experiments should investigate VEGFC and other vascular growth factors perhaps in combination with epithelial-targeted treatments. Ideally, these studies should include a slow-onset orthologous PKD1 model such as the *Pkd1*^{RC/RC} mouse,²⁴ since both of the models examined here progress very quickly which did not allow the examination of multiple stages of cyst initiation, progression and end-stage PKD. In addition, detailed studies need to be performed to determine optimal doses and timing periods for VEGFC treatment. Combining epithelial and endothelial therapies may generate the effective treatments urgently needed for these important human diseases.

Concise Methods

Animal models

Cys1^{cpk/+} (Jackson Laboratories, Bar Harbor, ME²⁰ and *Pkd1*^{nl/wt} heterozygous mice⁶ were bred to generate wild-type and homozygous littermates for analysis. *Cys1*^{cpk/+} were maintained on the C57BL/6J background for at least 25 generations and *Pkd1*^{nl/wt} on CD1 background for more than 10 generations. In some experiments, wild-type and homozygous *Cys1* and *Pkd1* mice were injected with either 100 ng/g body weight of recombinant VEGFC (R&D Systems Europe, Abingdon, UK) or vehicle (phosphate buffered saline) intraperitoneally daily. The daily volume administered was 20 µl, equivalent to providing 200 ml PBS to an adult human per day, or to an infant 20 ml/day. All animal procedures were approved by the UK Home Office.

Assessment of Renal Function

Blood was collected and blood urea nitrogen assessed using a commercially available assay kit, validated in mice.²⁵ Creatinine concentration was measured using isotope dilution electrospray mass spectrometry. Alanine aminotransferase was assessed using the Vitros 5600 clinical chemistry analyser (Ortho Clinical Diagnostics, High Wycombe, UK).

Histological Analysis and Immunohistochemistry

After anaesthesia, the vasculature was perfused to ensure optimal tissue preservation and maintain vessel patency with 1% paraformaldehyde (PFA) in PBS from a cannula inserted through the left ventricle into the aorta. Tissues were removed, fixed further by immersion in 1% PFA for another 1 hour, washed in PBS, dehydrated and embedded in wax; then five µm sections were cut. Some sections were stained with periodic acid Schiff reagent and haematoxylin to assess the overall histology. Pictures of whole stained kidneys were taken at low magnification under a dissecting microscope and the average area of individual cysts (defined as dilated tubules > 0.01 mm² in cross-sectional area) determined using ImageJ particle analysis (<http://rsbweb.nih.gov/ij/>).²⁶ Immunohistochemistry was performed for

CD206 (MCA2235T, AdB Serotec, Oxford, UK) with appropriate secondary antibodies conjugated to horseradish peroxidase and detected by 3,3'-diaminobenzidine with the colour development performed for the same duration of time for each sample. Negative controls consisted of omission of primary antibodies or substitution with preimmune serum.

Photomicrographs of 20 sequential fields using a $\times 20$ objective were taken and the area of the kidney cortex containing positive immuno-reactivity was analysed as a percentage of the whole image using ImmunoRatio and Image J software.²⁷ To circumvent any effects of cyst area on the analyses, the area occupied by dilated tubules $> 0.01 \text{ mm}^2$ was subtracted from each analysed image.

In some cases following perfusion, kidneys were prepared for cryosectioning by fixing in 1% PFA, placing samples in 30% sucrose in PBS and embedding in Tissue-Tek optimal cutting temperature compound (Sakura Finetek, Torrance, CA). Ten μm sections were permeabilised in PBS containing 0.03% Triton and then incubated in PBS-Triton containing 10% normal donkey serum (Jackson ImmunoResearch Laboratories Inc., West Grove, PA), 0.2% bovine serum albumin, and 0.1% sodium azide for 1 hour at room temperature to block non-specific antibody binding. Sections were incubated with 1 or more of the following primary antibodies overnight at room temperature: CD31 (MA3105, Thermo Fisher Scientific, Waltham, MA),^{28,29} galectin-3 (sc-20517, Santa Cruz Biotechnology, Inc., Dallas, Texas),³⁰ Ki67 (ab6155, Abcam, Cambridge, UK),²⁹ LYVE1 (AF2125, R&D Systems Europe),³¹ PDPN (ab11936, Abcam),³² PROX1 (11-022, AngioBio, Del Mar, CA),²⁸ VEGFR2 (AF644 R&D Systems Europe),³³ VEGFR3 (AF743, R&D Systems Europe).²⁸ Serial sections were used to determine co-localisation of vascular and lymphatic markers. After washing in PBS-Triton, sections were incubated with appropriate Cy3, AlexaFluor594 and AlexaFluor488 secondary antibodies and visualised by confocal microscopy. Images of whole kidney sections from fluorescent-labelled slides were obtained using an Axio Scan.Z1 (Carl Zeiss, Munich, Germany) and were then quantified in ImageJ. The area of the kidney sections positive for vascular markers was calculated as a percentage of the total DAPI⁺ area to circumvent any

effects of cysts on the analyses. The numbers of proliferating CD31⁺ and VEGFR3⁺ vessels were counted and expressed as positive cell numbers/cm² of DAPI area. To measure epithelial proliferation the number of Ki67⁺ cells were determined per 500 in at least 50 small cysts < 0.01 mm²; larger cysts > 0.01 mm² were also assessed. The average area occupied by LYVE1⁺/Prox1⁺ vessels was measured by analysing at least 20 vessels in each sample.

Immunoprecipitation and Western blotting

500 µg of protein from kidneys of *Pkd1^{nl/nl}* mice that were given vehicle or VEGFC was isolated using RIPA buffer and incubated with Dynabead Protein G (Life Technologies, Paisley, UK) and 5 µg of VEGFR3 (R&D Systems Europe) antibody. Bound protein was eluted, denatured and separated on sodium dodecyl sulfate-8% polyacrylamide gels. Following electroblotting, proteins were detected using antibodies for phosphotyrosine (05-321, Merck Millipore, Billerica, MA) or VEGFR3 (R&D Systems Europe). For the detection of endogenous VEGFC, 50 µg of kidney protein was separated, electroblotted and probed using a VEGFC antibody (sc-1881, Santa Cruz Biotechnology); α -tubulin was used as a house-keeping protein and densitometry analysis performed.

Real-Time Polymerase Chain Reaction (RT-PCR)

RNA was extracted using the RNeasy kit (Qiagen, Crawley, West Sussex, UK) from whole kidneys. 500 ng of RNA was used to prepare cDNA and quantitative RT-PCR was performed for *Arg1*, *Cd206*, *Col3a1*, *iNOS*, *Mcp1*, *Vegfa*, *Vegfc*, *Vegfr2* and *Vegfr3* on an CFX96 Touch Real-Time PCR Detection System (Bio-Rad Laboratories, Hemel Hempstead, UK) using SsoAdvanced Supermix (Bio-Rad Laboratories) with hypoxanthine-guanine phosphoribosyltransferase (*Hprt*) as a house-keeping gene. Fold-changes in gene expression were determined by the $2^{-\Delta\Delta CT}$ method. Primer details are available on request.

Statistics

All samples were assessed blinded to treatment. Data were presented as means \pm standard error of the mean (SEM). In experiments when differences between two groups were evaluated data was analysed by Mann-Whitney *U*-test (SPSS, Chicago, IL). When three or more groups were assessed one-way ANOVA with least square difference post-hoc test (SPSS) was used. Survival analysis was presented using the Kaplan-Meier estimate and assessed by the log rank test. Statistical significance was accepted at $p < 0.05$.

Acknowledgements

We thank UCL Biological Services, GOSH Chemical Pathology and Professor Neil Dalton (King's College London) for their assistance with animal experiments, alanine aminotransferase and creatinine measurements respectively. We thank Professor Paul Riley (University of Oxford) and Professor Paul Gissen (UCL Institute of Child Health) for helpful discussions regarding this work. This work was supported by a PhD studentship from Kids Kidney Research (to DAL, ASW and PJW); a project grant from Kidney Research UK (RP38/2013 to DAL and PJW) and a Bogue Research Fellowship to JLH. DAL is supported by a Kidney Research UK Senior Non-Clinical Fellowship (SF1/2008) and a Medical Research Council New Investigator Award (MR/J003638/1). The contributions by PB and DMcD were supported in part by grants from the National Heart, Lung, and Blood Institute (P01 HL024136 and R01 HL059157) of the US National Institutes of Health. KLP is supported by the ICH/GOSH Biomedical Research Centre. ASW acknowledges grant support from the Manchester Biomedical Research Centre.

Conflict of Interest Statement

JLH, PJDW and DAL hold a patent related to therapies targeting the lymphatics in polycystic kidney disease.

References

1. Harris PC, Torres VE: Polycystic kidney disease. *Annu Rev Med* 60: 321-337, 2009.
2. Wei W, Popov V, Walocha JA, Wen J, Bello-Reuss E: Evidence of angiogenesis and microvascular regression in autosomal-dominant polycystic kidney disease kidneys: a corrosion case study. *Kidney Int* 70: 1261-1268, 2006.
3. Bello-Reuss E, Holubec K, Rajaraman S: Angiogenesis in autosomal dominant polycystic kidney disease. *Kidney Int* 60: 37-45, 2001.
4. Tao Y, Kim J, Yin Y, Zafar I, Falk S, He Z, Faubel S, Schrier RW, Edelstein CL: VEGF receptor inhibition slows the progression of polycystic kidney disease. *Kidney Int* 72: 1358-1366, 2007.
5. Raina S, Honer M, Krämer SD, Liu Y, Wang X, Segerer S, Wüthrich RP, Serra AL: Anti-VEGF antibody treatment accelerates polycystic kidney disease. *Am J Physiol Renal Physiol* 301: F773-F783, 2011.
6. Lantinga-van Leeuwen IS, Dauwerse JG, Baelde HJ, Leonhard WN, van de Wal A, Ward CJ, Verbeek S, Deruiter MC, Breuning MH, de Heer E, Peters DJ: Lowering of Pkd1 expression is sufficient to cause polycystic kidney disease. *Hum Mol Genet* 13: 3069-3077, 2004.
7. Tammela T, Alitalo K: Lymphangiogenesis: Molecular mechanisms and future promise. *Cell* 140: 460-476, 2010.
8. Stan RV, Kubitza M, Palade GE: PV-1 is a component of the fenestral and stomatal diaphragms in fenestrated endothelia. *Proc Natl Acad Sci U S A* 96: 13203-13207, 1999.
9. Fine LG: Ernest Henry Starling (1866-1927) on the formation and reabsorption of lymph. *Nephron Physiol* 126: 9-17, 2014.
10. Huggenberger R, Ullmann S, Proulx ST, Pytowski B, Alitalo K, Detmar M: Stimulation of lymphangiogenesis via VEGFR-3 inhibits chronic skin inflammation. *J Exp Med* 207: 2255-2269, 2010.
11. Mäkinen T, Veikkola T, Mustjoki S, Karpanen T, Catimel B, Nice EC, Wise L, Mercer A, Kowalski H, Kerjaschki D, Stacker SA, Achen MG, Alitalo K: Isolated lymphatic endothelial

cells transduce growth, survival and migratory signals via the VEGF-C/D receptor VEGFR-3. *EMBO J* 20: 4762-4773, 2001.

12. Hamada K, Oike Y, Takakura N, Ito Y, Jussila L, Dumont DJ, Alitalo K, Suda, T: VEGF-C signaling pathways through VEGFR-2 and VEGFR-3 in vasculoangiogenesis and hematopoiesis. *Blood* 96: 3793-3800, 2000.

13. Kang DH, Hughes J, Mazzali M, Schreiner GF, Johnson RJ: Impaired angiogenesis in the remnant kidney model: II. Vascular endothelial growth factor administration reduces renal fibrosis and stabilizes renal function. *J Am Soc Nephrol* 12: 1448-1457, 2001.

14. Benedito R, Rocha SF, Woeste M, Zamykal M, Radtke F, Casanovas O, Duarte A, Pytowski B, Adams RH: Notch-dependent VEGFR3 upregulation allows angiogenesis without VEGF-VEGFR2 signalling. *Nature* 484: 110-114, 2012.

15. Karihaloo A, Koraihy F, Huen SC, Lee Y, Merrick D, Caplan MJ, Somlo S, Cantley LG: Macrophages promote cyst growth in polycystic kidney disease. *J Am Soc Nephrol* 22: 1809-1814, 2011.

16. Swenson-Fields KI, Vivian CJ, Salah SM, Peda JD, Davis BM, van Rooijen N, Wallace DP, Fields TA: Macrophages promote polycystic kidney disease progression. *Kidney Int* 83: 855-864, 2013.

17. Kanellis J, Fraser S, Katerelos M, Power DA: Vascular endothelial growth factor is a survival factor for renal tubular epithelial cells. *Am J Physiol Renal Physiol* 278: F905-F915, 2000.

18. Kaisaki PJ, Bergmann C, Brown JH, Outeda P, Lens XM, Peters DJ, Gretz N, Gauguier D, Bihoreau MT: Genomic organization and mutation screening of the human ortholog of Pkdr1 associated with polycystic kidney disease in the rat. *Eur J Med Genet* 51: 325-331, 2008.

19. Veron D, Reidy KJ, Bertuccio C, Teichman J, Villegas G, Jimenez J, Shen W, Kopp JB, Thomas DB, Tufro A: Overexpression of VEGF-A in podocytes of adult mice causes glomerular disease. *Kidney Int* 77: 989-999, 2010.

20. Hou X, Mrug M, Yoder BK, Lefkowitz EJ, Kremmidiotis G, D'Eustachio P, Beier DR, Guay-Woodford LM: Cystin, a novel cilia-associated protein, is disrupted in the cpk mouse model of polycystic kidney disease. *J Clin Invest* 109: 533-540, 2002.
21. Koch S, Claesson-Welsh L: Signal transduction by vascular endothelial growth factor receptors. *Cold Spring Harb Perspect Med* 2: a006502, 2012.
22. Outeda P, Huso DL, Fisher SA, Halushka MK, Kim H, Qian F, Germino GG, Watnick T: Polycystin signalling is required for directed endothelial cell migration and lymphatic development. *Cell Rep* 7: 634-644, 2014.
23. Coxam B, Sabine A, Bower NI, Smith KA, Pichol-Thievend C, Skoczylas R, Astin JW, Frampton E, Jaquet M, Crosier PS, Parton RG, Harvey NL, Petrova TV, Schulte-Merker S, Francois M, Hogan BM: Pkd1 regulates lymphatic vascular morphogenesis during development. *Cell Rep* 7: 623-633, 2014.
24. Hopp K, Ward CJ, Hommerding CJ, Nasr SH, Tuan HF, Gainullin VG, Rossetti S, Torres VE, Harris PC: Functional polycystin-1 dosage governs autosomal dominant polycystic kidney disease severity. *J Clin Invest* 122: 4257-4273, 2012.
25. Kolatsi-Joanou M, Price KL, Winyard PJ, Long DA: Modified citrus pectin reduces galectin-3 expression and disease severity in experimental acute kidney injury. *PLoS One* 6: e18683, 2011.
26. Chan SK, Riley PR, Price KL, McElduff F, Winyard PJ, Welham SJ, Woolf AS, Long DA: Corticosteroid-induced kidney dysmorphogenesis is associated with deregulated expression of known cystogenic molecules, as well as Indian hedgehog. *Am J Physiol Renal Physiol* 298: F346-F356, 2010.
27. Tuominen VJ, Ruotoistenmäki S, Viitanen A, Jumppanen M, Isola J: ImmunoRatio: a publicly available web application for quantitative image analysis of estrogen receptor (ER), progesterone receptor (PR) and Ki-67. *Breast Cancer Res* 12: R56, 2010.
28. Yao LC, Testini C, Tvorogov D, Anisimov A, Vargas SO, Baluk P, Pytowski B, Claesson-Welsh L, Alitalo K, McDonald DM: Pulmonary lymphangiectasia resulting from vascular

endothelial growth factor-C overexpression during a critical period. *Circ Res* 114: 806-822, 2014.

29. Dessapt-Baradez C, Woolf AS, White KE, Pan J, Huang JL, Hayward AA, Price KL, Kolatsi-Joannou M, Locatelli M, Diennet M, Webster Z, Smillie SJ, Nair V, Kretzler M, Cohen CD, Long DA, Gnudi L: Targeted glomerular angiotensin-1 therapy for early diabetic kidney disease. *J Am Soc Nephrol* 25: 33-42, 2014.

30. Chiu MG, Johnson TM, Woolf AS, Dahm-Vicker EM, Long DA, Guay-Woodford L, Hillman KA, Bawumia S, Venner K, Hughes RC, Poirier F, Winyard PJ: Galectin-3 associates with the primary cilium and modulates cyst growth in congenital polycystic kidney disease. *Am J Pathol* 169: 1925-1938, 2006.

31. Jeansson M, Gawlik A, Anderson G, Li C, Kerjaschki D, Henkelman M, Quaggin SE: Angiotensin-1 is essential in mouse vasculature during development and in response to injury. *J Clin Invest* 121: 2278-2289, 2011.

32. Danussi C, Spessotto P, Petrucco A, Wassermann B, Sabatelli P, Montesi M, Doliana R, Bressan GM, Colombatti A: Emilin1 deficiency causes structural functional defects of lymphatic vasculature. *Mol Cell Biol* 28: 4026-4039, 2008.

33. Lohela M, Heloterä H, Haiko P, Dumont DJ, Alitalo K: Transgenic induction of vascular endothelial growth factor-C is strongly angiogenic in mouse embryos but leads to persistent lymphatic hyperplasia in adult tissues. *Am J Pathol* 173: 1891-1901, 2008.

Figure Legends

Figure 1. Disorganisation of the renal microvasculature in *Pkd1^{nl/nl}* mice.

(A-E) Histology of kidneys obtained from *Pkd1^{wt/wt}* and *Pkd1^{nl/nl}* mice. Representative images of immunohistochemical staining for CD31 in the kidney of a one day old *Pkd1^{wt/wt}* (F) and *Pkd1^{nl/nl}* (G) mouse showing the microvasculature surrounding the tubules (*). Staining for VEGFR3 in one day old *Pkd1^{wt/wt}* (H) and *Pkd1^{nl/nl}* (I) mouse kidneys. Note that the CD31 and VEGFR3 frames shown for *Pkd1^{wt/wt}* and *Pkd1^{nl/nl}* mice are not of the same section. (J-M) Representative images of CD31 and VEGFR3 immunohistochemistry in three week old *Pkd1^{wt/wt}* and *Pkd1^{nl/nl}* mouse kidneys. (N-U) Double-labelling for CD31 and VEGFR3 in the same sections of *Pkd1^{wt/wt}* and *Pkd1^{nl/nl}* mice demonstrated co-localisation of both markers on vessels surrounding the kidney tubules. Bar is 50 μ m in each panel, g = glomerulus.

Figure 2. Administration of VEGFC to *Pkd1^{nl/nl}* mice improves kidney histology and function

(A) qRT-PCR comparing mRNA levels of *Vegfc* in *Pkd1^{wt/wt}* and *Pkd1^{nl/nl}* mouse kidneys at 7, 14 and 21 days after birth. All data is presented relative to levels in *Pkd1^{wt/wt}* kidney at day 7 where average expression was given an arbitrary value of 1. (B) Outline of experimental strategy. (C) VEGFR3 phosphorylation levels in the kidneys of *Pkd1^{nl/nl}* mice administered either vehicle or VEGFC. (D) Representative images showing overall appearance of kidneys from *Pkd1^{wt/wt}* and *Pkd1^{nl/nl}* mice administered either vehicle or VEGFC. Bar is 0.5 cm for each panel. (E) Assessment of kidney/body weight ratio. (F-I) Representative images of periodic-acid Schiff stained kidney sections obtained from *Pkd1^{wt/wt}* and *Pkd1^{nl/nl}* mice administered either vehicle or VEGFC, g = glomerulus, * = tubule (J) Analysis of average area of individual cysts. (K) Assessment of blood urea nitrogen, creatinine concentration (L) and serum alanine aminotransferase (M). (N-U) Histology of the heart, lung, liver and spleen from *Pkd1^{nl/nl}* mice administered either vehicle or VEGFC. n= 4-8 in each group and analyses, data is presented as mean \pm SEM. * = p <0.05, ** = p <0.01 and *** = p <0.001 between groups. Bar is 50 μ m in each panel.

Figure 3. VEGFC administration modulates the renal vasculature and reduces inflammation in *Pkd1^{nl/nl}* mice

Pkd1^{wt/wt} mice contained CD31⁺ and VEGFR3⁺ vessels arranged in a delicate linear network surrounding kidney tubules (indicated by * (A,B)); these vessels were disrupted in untreated *Pkd1^{nl/nl}* (C,D) whilst VEGFC administration to *Pkd1^{nl/nl}* mice normalised these aberrant patterns (E,F). (G-I) Immunostaining for CD206 positive cells revealed prominent expression in the interstitial tissue surrounding cysts (*), but not in glomeruli (g) in *Pkd1^{nl/nl}* mice which was diminished following VEGFC therapy. Quantification of CD206 (J) positive cells, n = 5-8 in each group. mRNA levels of *Mrc1* (K), *Arg1* (L), *iNOS* (M), *Mcp1* (N) and *Col3a1* (O) assessed by quantitative real-time PCR and presented relative to levels in *Pkd1^{wt/wt}* kidneys, n=4 in each group (P, Q). Double-labelling in three week old *Pkd1^{nl/nl}* mice administered vehicle with antibodies to detect either VEGFR2 or VEGFR3 and galectin-3, a marker for cyst epithelial cells derived from the collecting duct (arrows). All data is presented as mean ± SEM. * = p <0.05, ** = p <0.01, *** = p <0.001 between groups. Bar is 50 µm in each panel.

Figure 4. VEGFC treatment improves kidney histology and survival in *Cys1^{cpk/cpk}* mice

(A) Outline of experimental strategy. (B) Representative images showing overall appearance of kidneys from *Cys1^{+/+}* and *Cys1^{cpk/cpk}* mice administered either vehicle or VEGFC. Bar is 0.5 cm for each panel. (C) Assessment of kidney/body weight ratio and (d) blood urea nitrogen concentration. (E-H) Representative images of periodic-acid Schiff stained kidney sections obtained from *Cys1^{+/+}* and *Cys1^{cpk/cpk}* mice administered either vehicle or VEGFC. Bar is 50 µm in each panel, g= glomerulus, * = dilated tubule. (I) Image J particle analysis of images of whole kidneys under a dissection microscope to determine the average area of individual cysts. (J) Survival analysis of *Cys1^{cpk/cpk}* mice administered either vehicle or VEGFC. n = 7-11 in each group for a-i, n = 6 for j, data is presented as mean ± SEM, * = p <0.05, ** = p <0.01, *** = p <0.001 between groups.

Figure 1

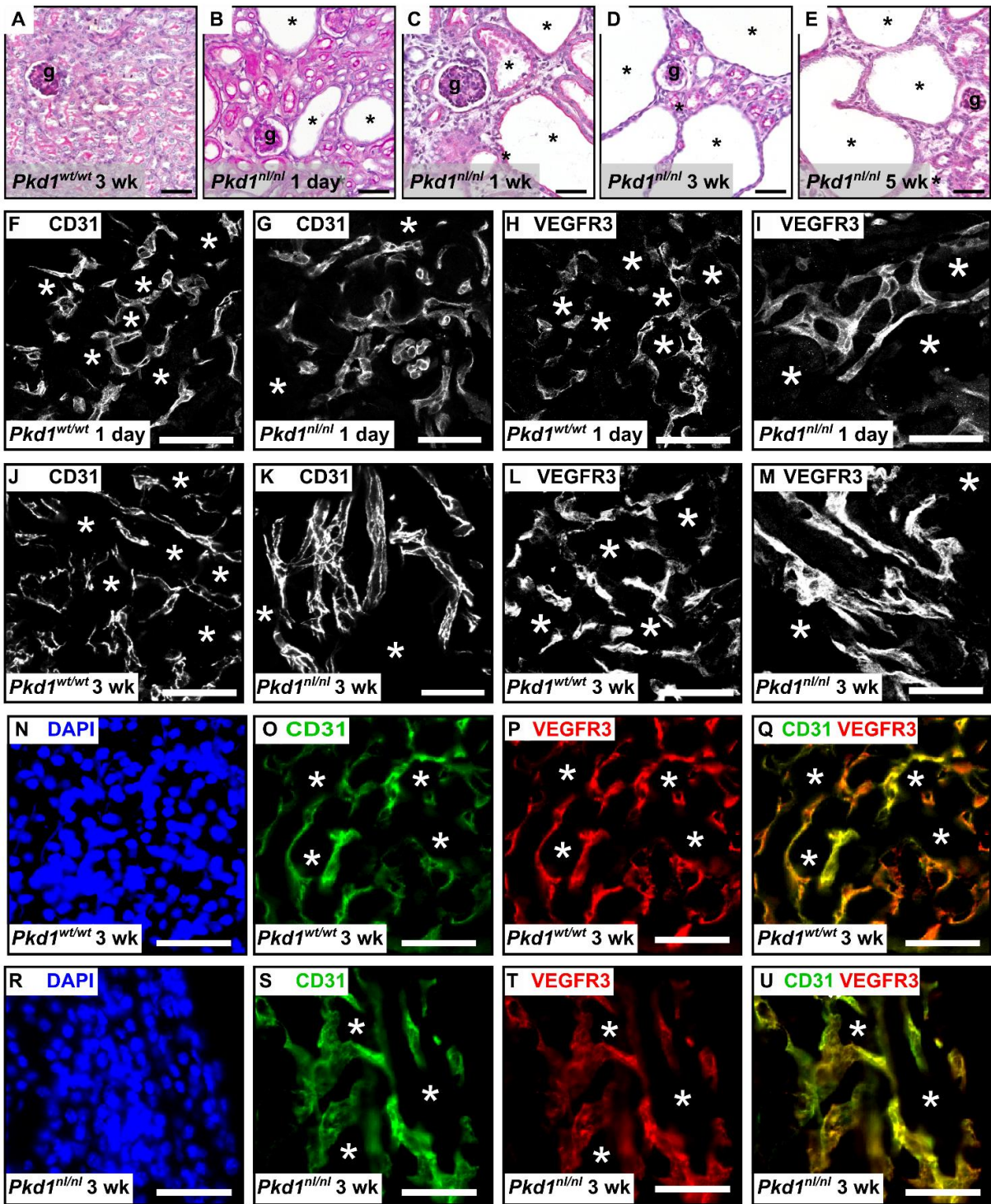


Figure 2

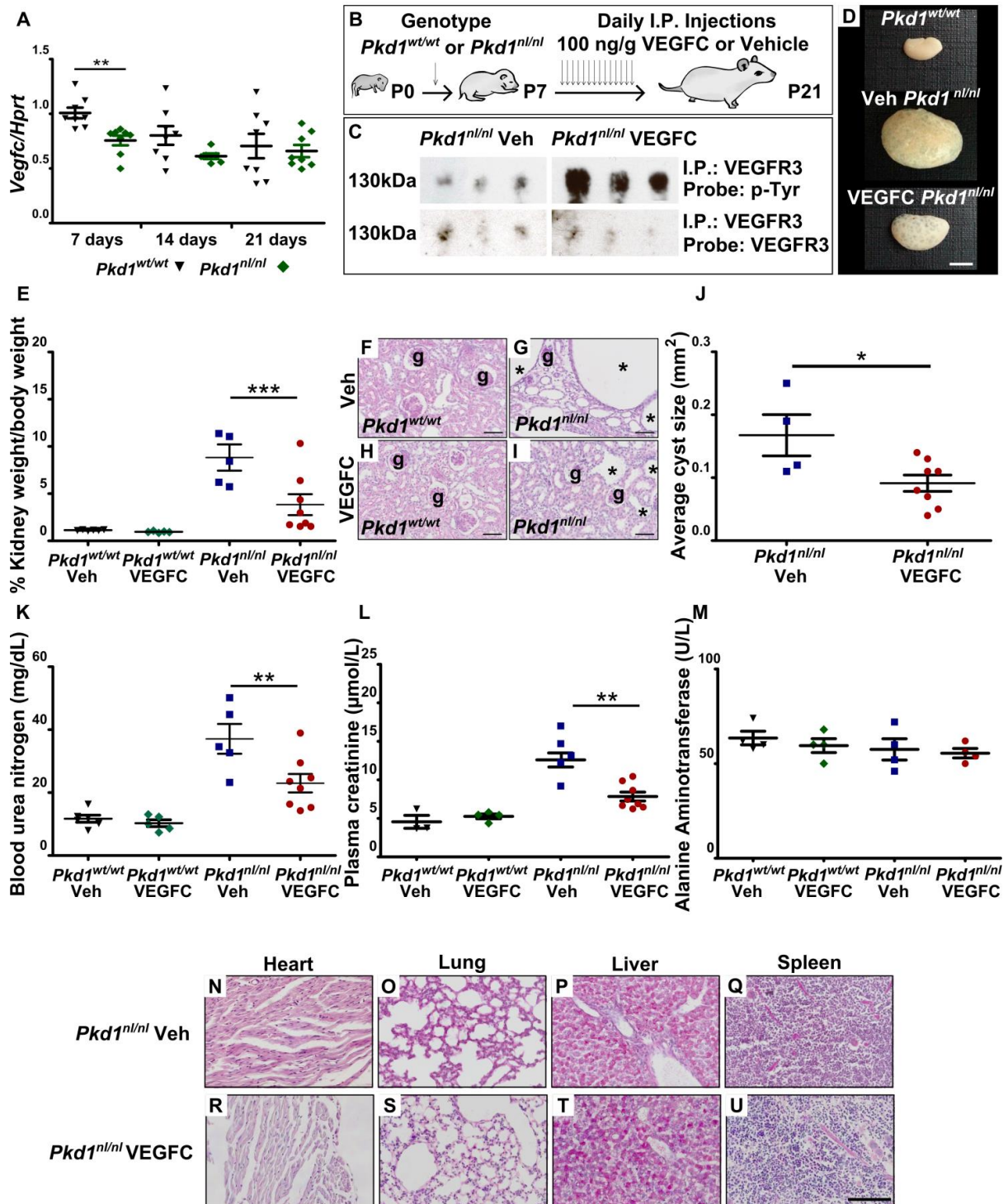


Figure 3

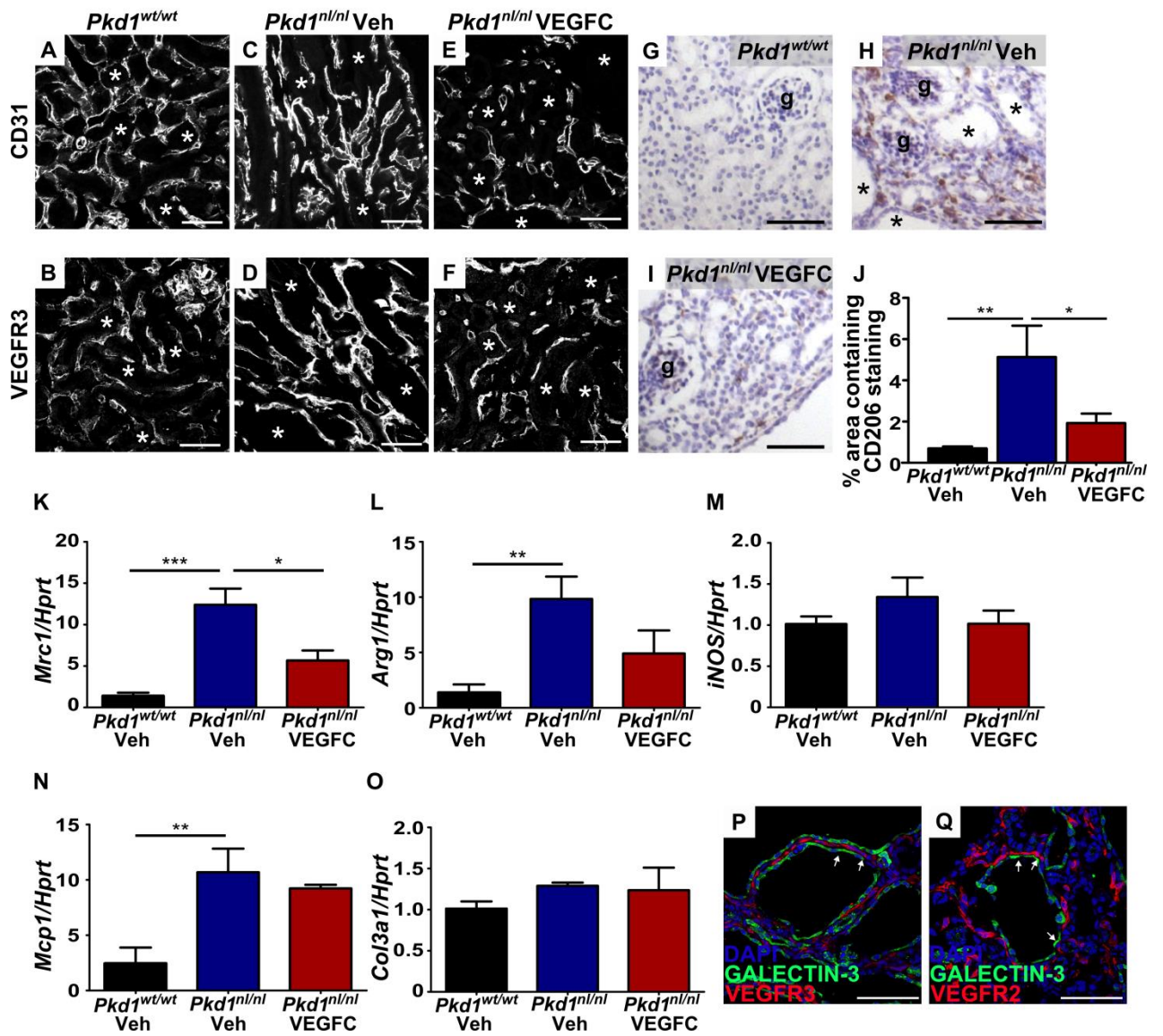
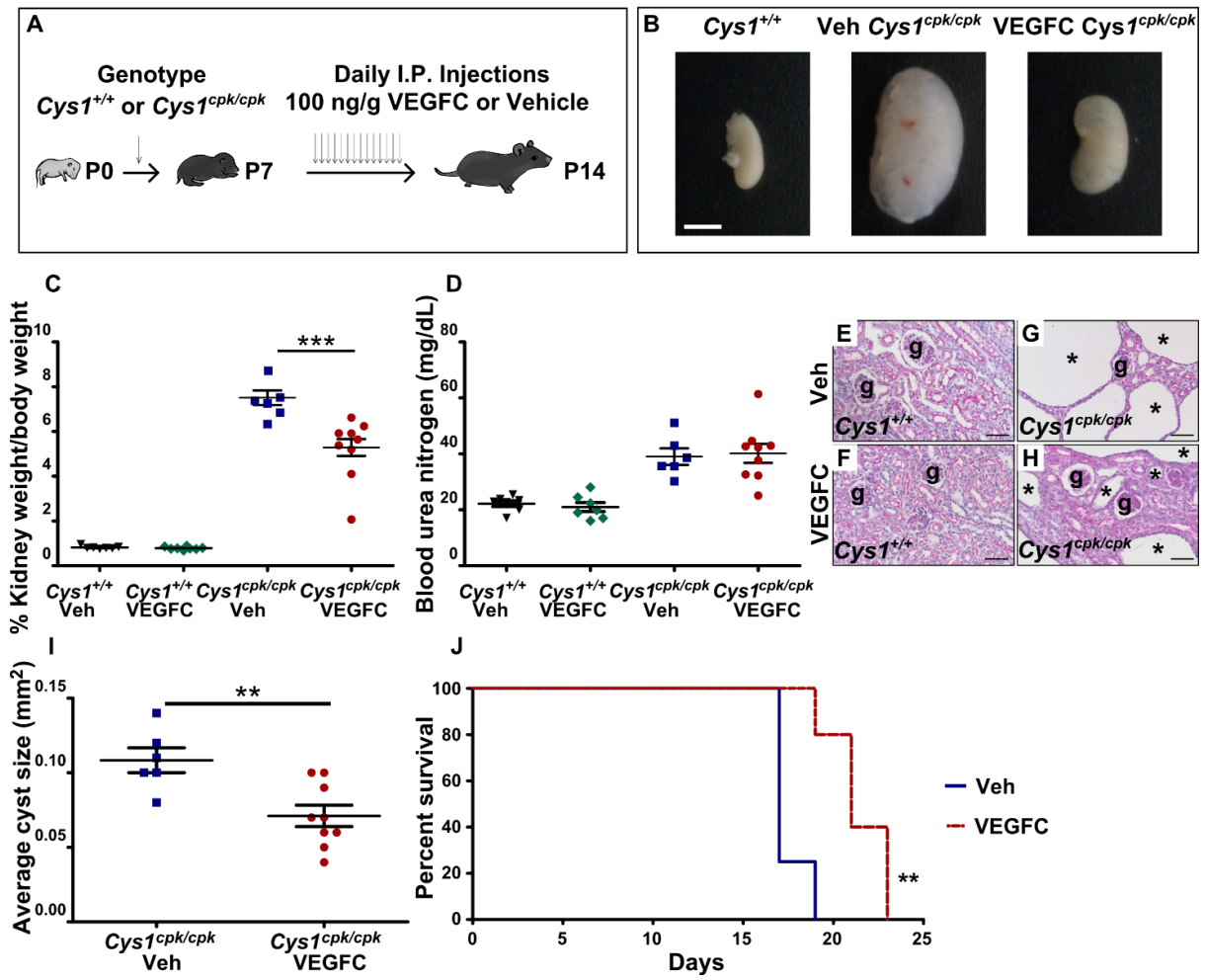
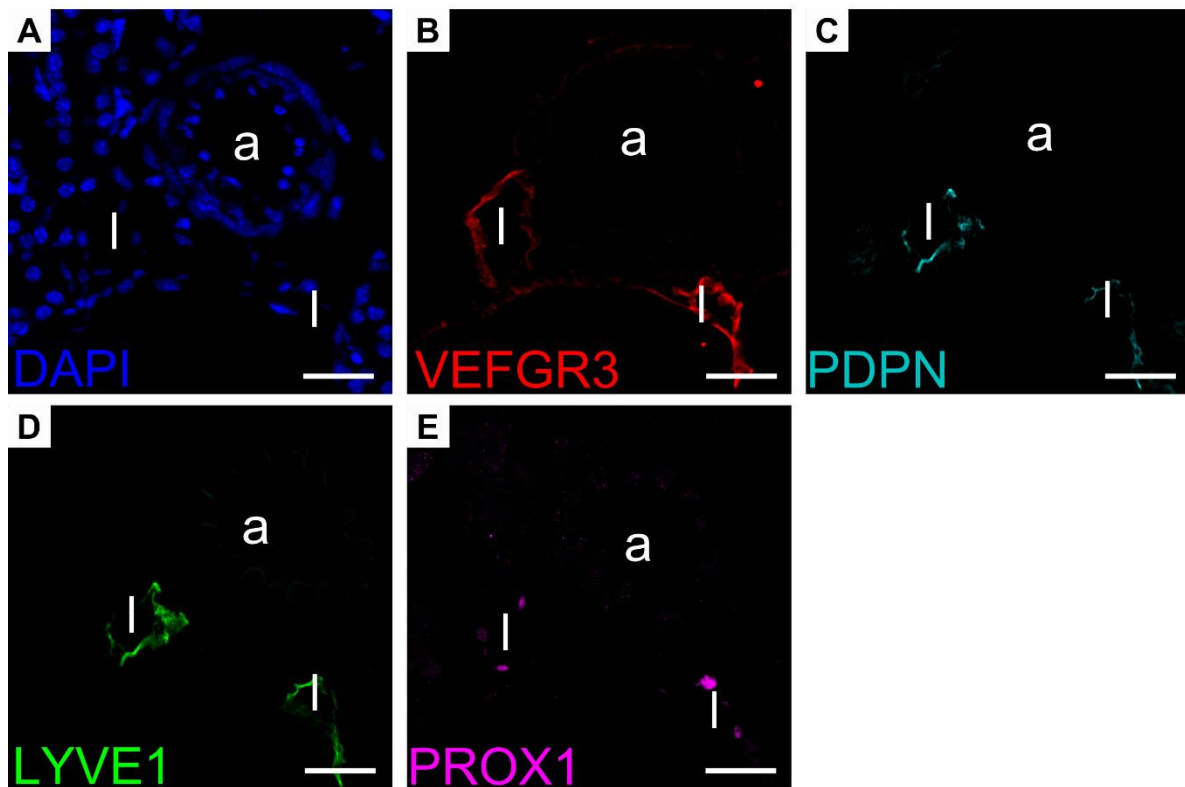


Figure 4



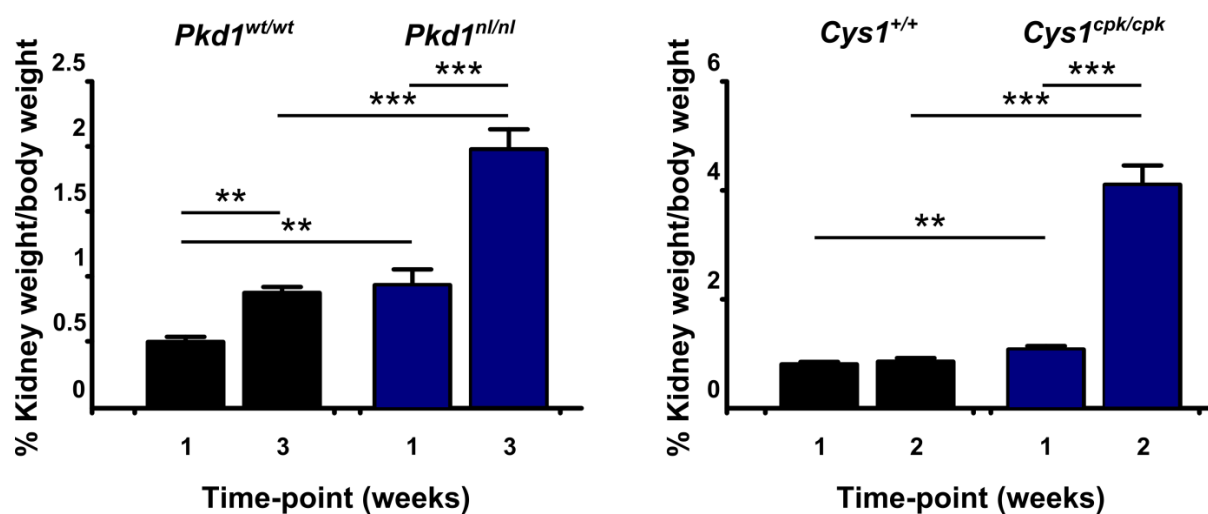
Supplementary figure 1



Supplementary Figure 1. Expression of lymphatic markers in *Pkd1*^{wt/wt} mice

VEGFR3 (B), PDPN (C), LYVE1 (D) and PROX1 (E) co-localised to the larger lymphatics (l) in the kidneys of three week old *Pkd1*^{wt/wt} mice. None of the markers were detected in the arteries (a) of the kidney. Bar is 50 μm in all panels.

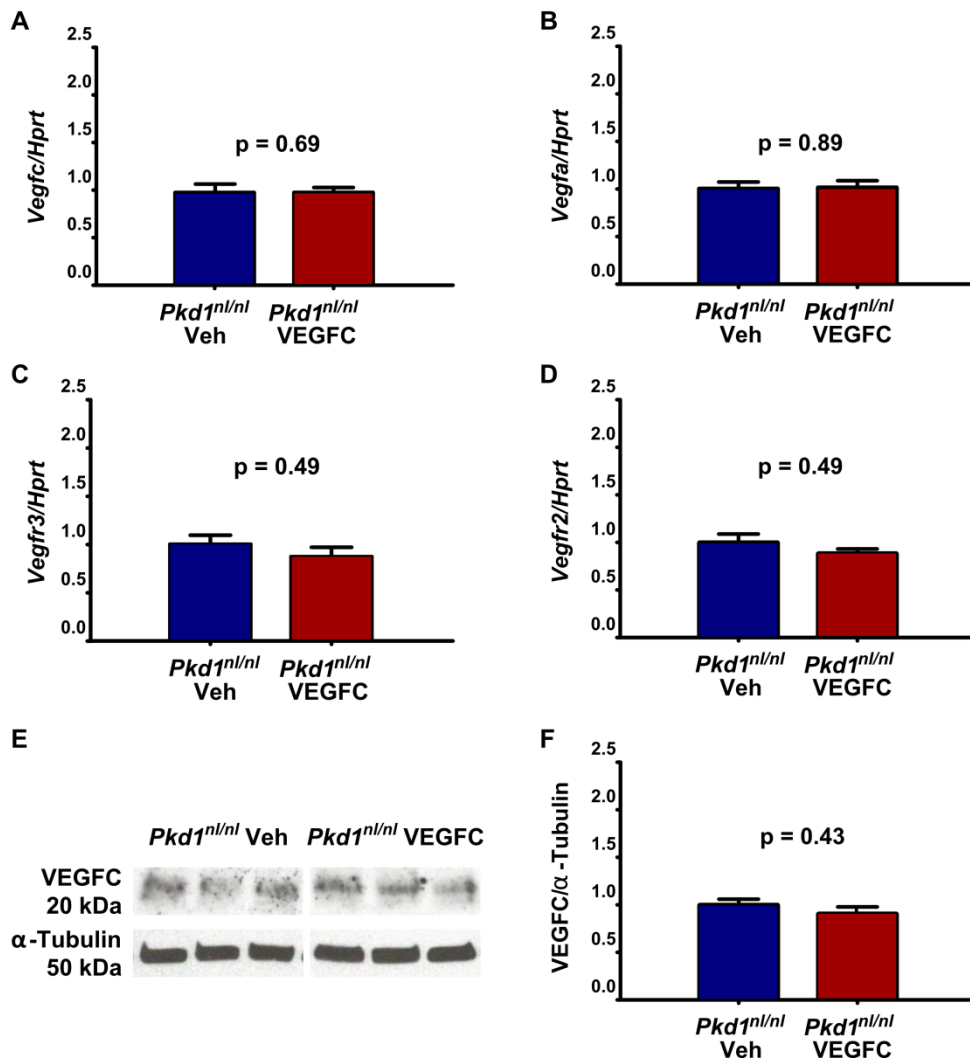
Supplementary figure 2



Supplementary Figure 2. Percentage of kidney weight/body weight in *Pkd1*^{nl/nl} and *Cys1*^{cpk/cpk} mice

The kidneys of *Pkd1*^{nl/nl} mice grew rapidly during 1 to 3 weeks of age, the period when VEGFC treatment was provided, with only a modest growth in *Pkd1*^{wt/wt} kidney (n=4-9 in each group and time-point). Rapid kidney growth occurred during weeks 1 to 2 of age in *Cys1*^{cpk/cpk} when VEGFC was administered, with no change in *Cys1*^{+/+} mice during this period (n=13-17 in each group and time-point). All data is presented as mean \pm SEM. ** = p < 0.01, *** = p < 0.001 between groups.

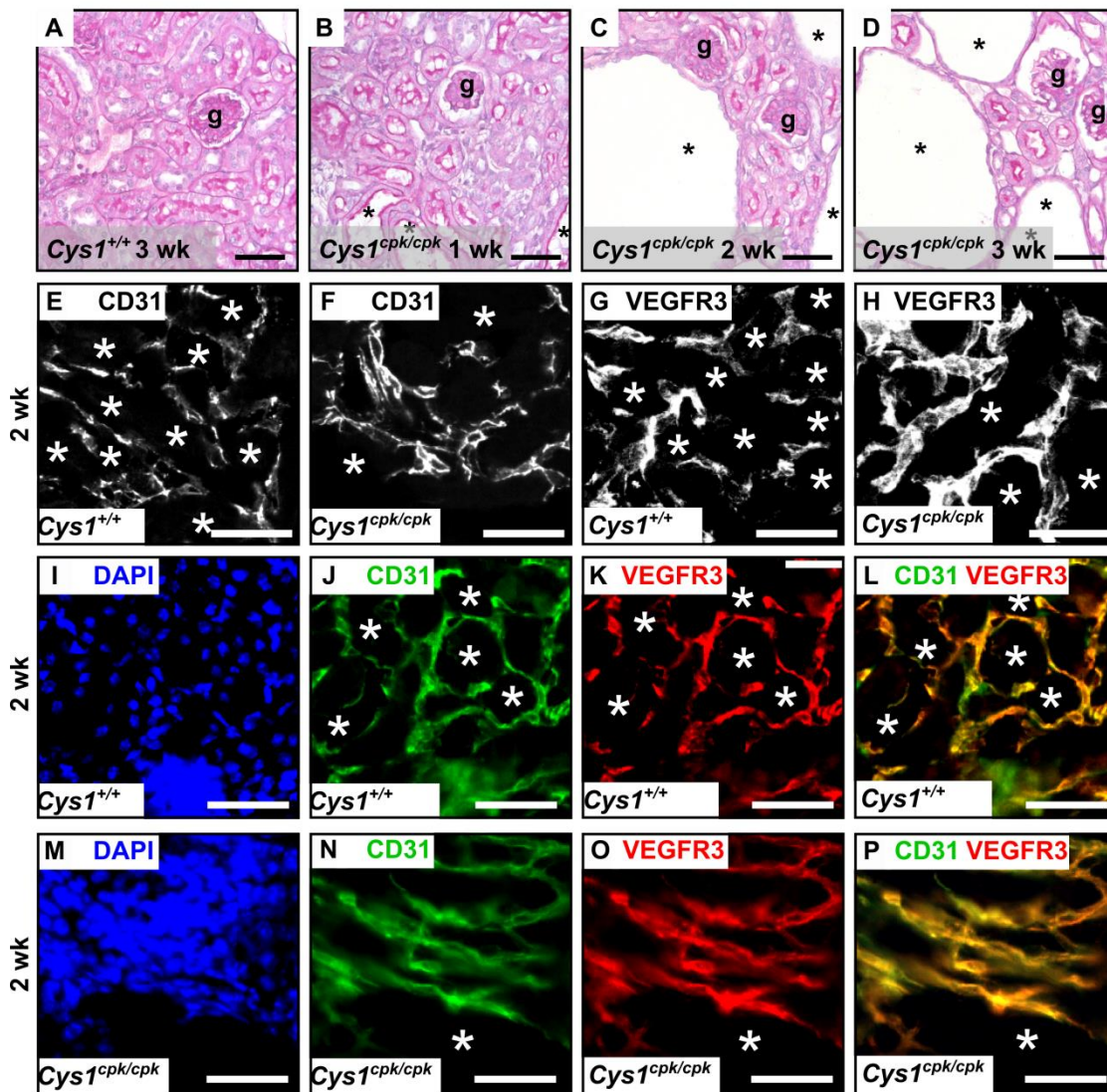
Supplementary figure 3



Supplementary Figure 3. Endogenous Vegfa, Vegfc, Vegfr2 and Vegfr3 levels were not altered in the kidneys of *Pkd1^{nl/nl}* mice following VEGFC treatment

qRT-PCR comparing mRNA levels of *Vegfa* (A), *Vegfc* (B), *Vegfr2* (C) and *Vegfr3* (D) in *Pkd1^{nl/nl}* mouse kidneys following either vehicle (PBS) or VEGFC treatment (n=4 in each group). (E) Western blotting for VEGFC in *Pkd1^{nl/nl}* mouse kidneys following either vehicle (PBS) or VEGFC treatment (n=3 in each group). Densitometry was performed (F) using α -tubulin as a house-keeping protein. All data is presented as mean \pm SEM and presented relative to levels in *Pkd1^{nl/nl}* kidneys administered PBS where average expression was given an arbitrary value of 1.

Supplementary figure 4



Supplementary Figure 4. Disorganisation of the renal microvasculature in *Cys1^{cpk/cpk}* mice.

(A-D) Histology of kidneys obtained from *Cys1^{+/+}* and *Cys1^{cpk/cpk}* mice. Representative images of immunohistochemical staining for CD31 in the kidney of a two week old *Cys1^{+/+}* (E) and *Cys1^{cpk/cpk}* (F) mouse showing the positive vessels surrounding the tubules (*). Staining for VEGFR3 in two week old *Cys1^{+/+}* (G) and *Cys1^{cpk/cpk}* (H) mouse kidneys. Note that the CD31 and VEGFR3 frames shown for *Cys1^{+/+}* and *Cys1^{cpk/cpk}* mice are not of the same section. (I-P) Double-labelling for CD31 and VEGFR3 in the same sections of *Cys1^{+/+}* and *Cys1^{cpk/cpk}* mice demonstrated co-localisation of both markers on vessels surrounding

the kidney tubules. Bar is 50 μm in each panel, g = glomerulus.

Supplementary Table 1: Quantification of vascular parameters in the kidneys of *Pkd1^{wt/wt}* and *Pkd1^{nl/nl}* mice administered PBS or VEGFC.

	<i>Pkd1^{wt/wt}</i>	<i>Pkd1^{nl/nl}</i> PBS	<i>Pkd1^{nl/nl}</i> VEGFC
% area positive for CD31	32.0 ± 1.5	44.2 ± 1.8 ^a	33.5 ± 2.4 ^b
CD31 ⁺ Ki67 ⁺ cells/cm ² of DAPI area	48.7 ± 6.0	13.9 ± 1.5 ^a	38.4 ± 4.9 ^b
Average size of LYVE1 ⁺ Prox1 ⁺ (µm ²)	6.8 ± 0.4	7.0 ± 0.9	9.1 ± 0.6 ^b
% area positive for VEGFR3	19.8 ± 2.1	38.4 ± 1.3 ^a	24.4 ± 2.0 ^b
VEGFR3 ⁺ Ki67 ⁺ cells/cm ² of DAPI area	44.9 ± 3.7	17.0 ± 1.6 ^a	54.1 ± 13.4 ^b

Data is presented as mean ± SEM. n=3-6 three week old mice per group. a = p <0.05 comparing *Pkd1^{wt/wt}* with *Pkd1^{nl/nl}* mice administered PBS, b = p <0.05 comparing *Pkd1^{nl/nl}* mice administered PBS or VEGFC.

Supplementary Table 2: Quantification of vascular parameters in the kidneys of *Cys1^{+/+}* and *Cys1^{cpk/cpk}* mice administered PBS or VEGFC.

	<i>Cys1^{+/+}</i>	<i>Cys1^{cpk/cpk}</i> PBS	<i>Cys1^{cpk/cpk}</i> VEGFC
% area positive for CD31	40.8 ± 1.8	44.6 ± 0.3	41.3 ± 1.2
CD31 ⁺ Ki67 ⁺ cells/cm ² of DAPI area	66.4 ± 6.4	20.3 ± 4.8 ^a	40.9 ± 5.2 ^b
Average area of LYVE1 ⁺ Prox1 ⁺ vessels (µm ²)	2.9 ± 0.3	4.0 ± 0.5	5.0 ± 0.2
% area positive for VEGFR3	35.3 ± 2.2	43.1 ± 0.4 ^a	38.7 ± 1.6 ^b
VEGFR3 ⁺ Ki67 ⁺ cells/cm ² of DAPI area	54.8 ± 5.6	22.7 ± 3.0 ^a	38.8 ± 2.5 ^b

Data is presented as mean ± SEM. n=3-5 two week old mice per group. a = p <0.05 comparing *Cys1^{+/+}* with *Cys1^{cpk/cpk}* mice administered PBS, b = p <0.05 comparing *Cys1^{cpk/cpk}* mice administered PBS or VEGFC.